JOURNAL OF MATERIALS SCIENCE **36** (2001) 2019–2026

Hydrothermal synthesis of lead doped barium titanate

R. E. VOLD, R. BIEDERMAN, G. A. ROSSETTI JR.[‡], A. SACCO JR.*
Center for Advanced Microgravity Materials Processing, Department of Chemical Engineering, Northeastern University, Boston, MA 02115, USA
E-mail: rvold@lynx.neu.edu

T. SJODIN
Department of Physics, Northeastern University, Boston, MA 02115, USA

A. RZHEVSKII
Department of Chemical Engineering, Worcester Polytechnic Institute, Worcester, MA 01609, USA

Lead doped barium titanate was synthesized hydrothermally at 363 K for 140 h. A molar formula of $Ba_{(1-x)}Pb_xTiO_3$ was used, where x ranged between 0.025 and 0.75. The crystal structure, phase purity, and particle morphology was investigated by x-ray diffraction, Raman spectroscopy and electron microscopy. Under the synthesis conditions used, lead (Pb^{2+}) was shown to incorporate into the perovskite structure when the dopant was kept below 20%. Above 20% Pb, other phases appeared and at 75% Pb no reaction to the perovskite structure took place. Unexpectedly, barium titanate containing from 2.5% Pb to 10% Pb appeared to be of orthorhombic symmetry. This was concluded by total pattern fitting of x-ray diffraction profiles and from splitting of the 222 reflection. The factors controlling the tendency for these materials to adopt orthorhombic symmetry as opposed to the more commonly observed tetragonal or cubic symmetries are briefly discussed.

1. Introduction

Since the discovery of its high dielectric constants in the mid nineteen forties, ferroelectric barium titanate ($BaTiO_3$) has been an important member of the U.S. electronic ceramics market, which is expected to total $6.3 billion in the year 2001 [1]. $BaTiO_3$ has found extensive use in the ceramic capacitor industry. It is ferroelectric below 403 K, and goes through three phase transitions upon cooling [2]. At 403 K the cell transforms from cubic to tetragonal, and at 273 K the face-diagonal elongates to form an orthorhombic phase. Below 189 K the body diagonal elongates, resulting in a rhombohedral cell [2].

Traditionally, barium titanate has been produced by conventional solid state reaction techniques. However, in recent years there has been a trend towards the use of chemical methods. One such method is hydrothermal synthesis, which involves the treatment of aqueous solutions at moderate temperatures and pressures. The hydrothermal processing of $BaTiO_3$ takes place in a highly alkaline environment ($pH > 12$), and usually provides fine and monodisperse particles ranging from 100 nm to 400 nm in size [3]. It makes the fine powders useful in production of thin dielectric layers [3, 4].

Various workers [3–14] have prepared $BaTiO_3$ hydrothermally using temperatures ranging from 343 K to 773 K and reaction times of 2 h–140 h. In most of these syntheses the authors reported cubic $BaTiO_3$ powders at room temperature, although Christensen and Rasmussen [15] reported that the tetragonal phase could be directly synthesized hydrothermally at 723 K–873 K. The tetragonal form is the thermodynamically stable symmetry observed for large particles at room temperature, and normally the cubic phase would only be observed above the Curie temperature (T_c) of 403 K [8]. However, some studies [6, 18] suggest a correlation between the destabilization of the thermodynamically favored tetragonal phase at room temperature and the crystallite size of these particles. In addition, impurities such as hydroxyl defects, and their associated lattice distortions, may also play a role in destabilizing the tetragonal phase.

The influence of particle size on the room-temperature tetragonality distortion has been studied by a number of authors [12, 13, 16, 17]. Begg *et al.* [16] reported that $BaTiO_3$ crystallites $\leq$190 nm in size were cubic, while particles $\geq$270 nm were completely tetragonal at room temperature. Uchino *et al.* [12] found

*Author to whom all correspondence should be addressed.
‡*Present Address*: Continuum Control Corporation, 45 Manning Park, Billerica, MA 01821, USA.

the cubic particles to be stable below 120 nm, and noticed a similar trend to Begg *et al.* showing decreasing tetragonal distortion with smaller particles. Similarly, Li and Shih [13] noted small particles that would normally be cubic when isolated, could be tetragonal if aggregated into a cluster. The average particle size was reported as 150 nm and the average cluster size as 900 nm [13]. On the contrary, Arlt *et al.* [17] found that fine $BaTiO_3$ particles exhibited a mixture of tetragonal and orthorhombic symmetry below 150 nm in size, and below 50 nm the structure was reported to be orthorhombic.

In hydrothermally prepared powders, the presence of impurities such as H_2O and OH^- defects and their associated lattice distortions, are well known to reside within the $BaTiO_3$ structure. It is believed that these defects impact the thermodynamically favored $BaTiO_3$ symmetry at room temperature. The hydroxyl defects are related to the processing conditions, and are usually confirmed by Fourier Transform-Infrared (FT-IR) spectroscopy. According to Vivekananden and Kutty [5] the residual hydroxyl ions in the oxygen sites probably result in defects that are compensated for by cation vacancies, resulting in lattice strains that might upset the long range polar ordering that drives the cubic-tetragonal transformation on cooling [18]. That is, the metastable cubic phase might appear from high concentrations of hydroxyl defects, rather than certain size-effects. Additionally, the feedstock molar ratio of Ba/Ti has been shown to influence relative phase stabilities. Shi *et al.* [7] found that a molar ratio of Ba : Ti = 1 resulted in a cubic product. In contrast, increasing the Ba : Ti ratio to three lead to a tetragonal phase. It was also confirmed by Shi *et al.* that the cubic phase had a higher concentration of hydroxyl defects compared to the tetragonal form [7]. Dutta and Gregg [6] showed that doping $BaTiO_3$ with Cl^- lead to stabilization of the tetragonal phase at room temperature. They suggested that the chloride ions assist in the nucleation of the larger crystals and the smaller crystals act as seed nuclei.

A number of factors seem to contribute to the destabilization of the tetragonal symmetry in $BaTiO_3$, but there is still no clear consensus as to the origin. Due to the openness of the ABO_3 perovskite structure, barium titanate can incorporate other ions into the A- or B-lattice sites (tolerance factor, $\tau = 1.06$). These ion substitutions are another way to influence phase stabilities in fine particles.

In the present study, the effects of doping $BaTiO_3$ with lead (Pb^{2+}) were investigated. It was hypothesized that the substitution of Pb^{2+} for Ba^{2+} might help stabilize the tetragonal phase. Because the Pb^{2+} is a Rydberg ('lone-pair') ion, it was expected to produce lattice distortions. It is known that substitution of Pb^{2+} for Ba^{2+} decreases the a-lattice parameter while increasing the c-lattice parameter. As a result, the c/a ratio of $BaTiO_3$ is only 1.01, while that for $PbTiO_3$ ($c = 4.150$ Å, $a = 3.899$ Å) is 1.065 [19]. Additionally, the Curie temperature of Pb-doped $BaTiO_3$ was expected to increase, based on the Tc of $PbTiO_3$ (763 K) [20]. It is also known that compositions in the $PbTiO_3 : BaTiO_3$ system form a complete homogeneous solid solution when synthesized by conventional high temperature methods. In order to investigate the characteristics of hydrothermally prepared compositions of the $PbTiO_3 : BaTiO_3$ system, barium hydroxide octahydrate, anatase, lead subacetate and double distilled de-ionized (DI) water were reacted under autogenous conditions at 363 K for 140 h. A molar formula of $Ba_{(1-x)}Pb_xTiO_3$ was used, where x ranged between 0.025 and 0.75. Pure $BaTiO_3$ was also synthesized hydrothermally at 363 K for 140 h, using five percent excess barium in the starting reaction mixture, for comparison to the lead doped $BaTiO_3$ samples.

All of the samples were analyzed by powder x-ray diffraction (XRD) and Raman spectroscopy to determine the crystallinity, structural characteristics and phase purity. Scanning electron microscopy (SEM) was also utilized to study the morphology and the size effects of the particles. Particle size distribution (PSD) measurements were used as a confirmation tool in determining the size distributions.

2. Experimental procedure

The following hydrothermal synthesis procedure was adapted from the work of Eckert *et al.* [14]. The samples were prepared using Ba : Ti molar ratios of 1 : 1 and 1.05 : 1.00. An excess of five-percent barium was used in an attempt to drive the reaction to completion.

Reagent-grade $Ba(OH)_2{\cdot}8H_2O$ (98+%, Aldrich Chemical, Milwaukee, WI) and well crystallized anatase (99.8% metals basis, Alfa Division, Danvers, MA) powders, were measured into a 60 ml teflon reaction vessel (Sauvillex Corp., Minnetonka, Minnesota). Double distilled DI water (18.5 MOhm @298 K) was added to the mixture, and the vessel was sealed and shaken for 30s to allow for mixing. The vessel was then placed in a 363 K oven (Gallenkamp Oven, 300Plus Series) and held at temperature for 140 h.

After completion of the reaction, the mixture was stirred and poured into a beaker, while still hot, and diluted with 100 ml 1M formic acid (Aldrich Chemical). The formic acid rinse was performed to remove unreacted and residual barium hydroxide along with potential carbonates, such as $BaCO_3$. The solution was then stirred for one minute using a magnetic stirrer and stirplate. Afterwards the solution was vacuum filtered under ambient conditions, using a 0.2 μm Supor200® filter-membrane (Gelman Sciences, Ann Arbor, Michigan). Three filter-membranes were required for each sample, due to the large product masses. Approximately 100 ml of DI water was utilized to wash the product (on each filter-membrane) during the filtration. The resulting filter cakes were placed in a 363 K oven for 12 h.

The same procedure, as described above, was employed in the synthesis of lead doped barium titanate. $Ba_{(1-x)}Pb_xTiO_3$, with x ranging from 0.025 to 0.75, was prepared using lead subacetate, $(CH_3CO_2)_2Pb{\cdot}2Pb(OH)_2$ (Aldrich Chemical) as the lead source. In each of the Pb-doped samples, the addition of anatase was kept the same as for the pure $BaTiO_3$ sample (6.26×10^{-2} moles). All of the lead additions were based on moles of PbO. To determine the PbO content, lead subacetate was assayed by gravimetry upon ignition in air at 1073 K. The lead oxide concentration measured in this way was 78.0%.

The dried powders were analyzed at room temperature utilizing a Siemens D5005 Bragg-Brentano diffractometer (Siemens, Karlsruhe, Germany), using Cu K_α radiation. The diffractometer was equipped with a curved graphite crystal diffracted beam monochromator and a NaI scintillation detector. The operating conditions were 45 kV and 30 mA, using either a 0.1 mm or 0.2 mm receiving slit and a 1° or 0.5° divergence slit. Steps of 0.01° 2θ and a count time of 1s was used in most of the x-ray scans.

An Aerosizer LD (Amherst Process Instruments Inc., Hadley, MA) was used to measure the particle size distributions of the dried powders. The time-of-flight for a single particle was measured using two laser beams [21]. The time-of-flight data were related to the geometric diameter of the particles [21], using the known theoretical density of the particles. The theoretical density for the mixed system, $Ba_{1-x}Pb_xiO_3$, was based on an average value of the weight percentages of the compounds multiplied by their respective densities. Each sample was run for 200 s and it resulted in a count of ca. 4.5×10^5 particles. The density of barium titanate (6.012 g/cm^3) was used for the calculations. The morphology of the products was observed using a scanning electron microscope (JEOL JSM Model 840). An electron beam of 15 keV was used to generate the micrographs.

Several specimens were examined by Raman spectroscopy to establish the local symmetry of the products. Because of the fine particles, it was not possible to completely determine the symmetry solely on the basis of XRD data. Two different Raman set-ups were used to acquire the data. In one set-up, Raman data was collected at room temperature for pure barium titanate (Ba : Ti = 1.05 : 1.00) and the sample doped with 10% Pb, using a Spex 1870B spectrometer. The samples were excited with the 413.1 nm line and each spectrum was measured using a 180° back-scattering geometry and a Kr-ion laser power of 4 mW. The second set of Raman data was collected on a Spex 1877 Triplemate Triple Spectrometer using an ultra-low-light sensitive Model 2601B Mepsicron-Single-Photon imaging detector at an excitation wavelength of 244 nm. Each spectrum was collected for about 3 hrs using an Ar-ion laser power of ∼2 mW and a 180° back-scattering geometry.

3. Results and discussion

The synthesis procedure described above resulted in product yields of about 96 mol% based on the conversion of barium hydroxide. Product mass and mole-balances determined the yield. As expected, the sample produced from the reaction mixture containing excess barium (Ba : Ti = 1.05 : 1.00) had less anatase. This barium titanate (Ba : Ti = 1.05 : 1.00) sample was also well crystallized and compared to commercially available barium titanate from Sigma-Aldrich Chemical Company (99.995%), as seen in Fig. 1. The peak widths and intensities of the two series of patterns are qualitatively very similar. For the hydrothermally synthesized sample, however, there is a relatively small peak located at ∼26° 2θ, which is indicative of unreacted anatase. Fig. 1 also shows the pattern of commercial $BaTiO_3$ after calcination at 1473 K for 2 h. The tetrgonal splitting of the 002/200 reflection is more obvious for this pattern, because the high temperature treatment increases the degree of crystallinity.

The 002/200 reflections of the hydrothermally derived barium titanate sample were fitted using a Pseudo-Voigt profile function to determine the lattice parameters. The areas of the peaks (002/200) were constrained to be in a 1 : 2 ratio, consistent with the tetragonal symmetry [22, 23]. The lattice parameters so obtained

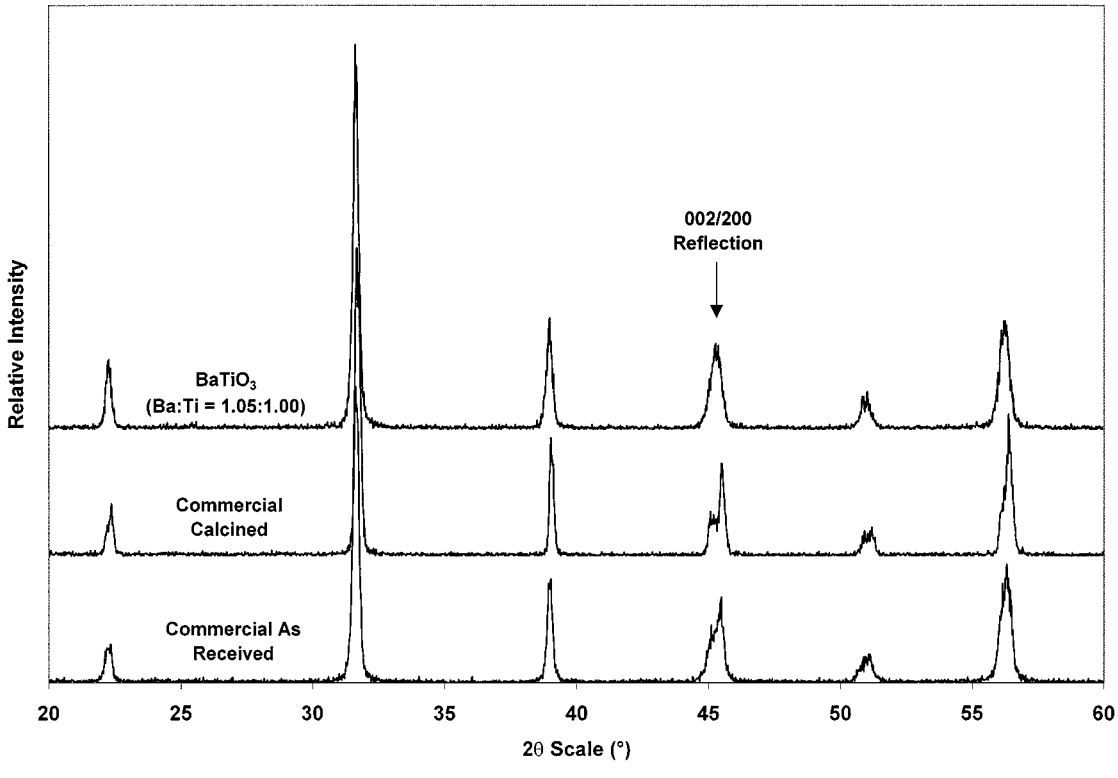

Figure 1 X-ray diffraction data of pure barium titanate compared to a commercial barium titanate sample.

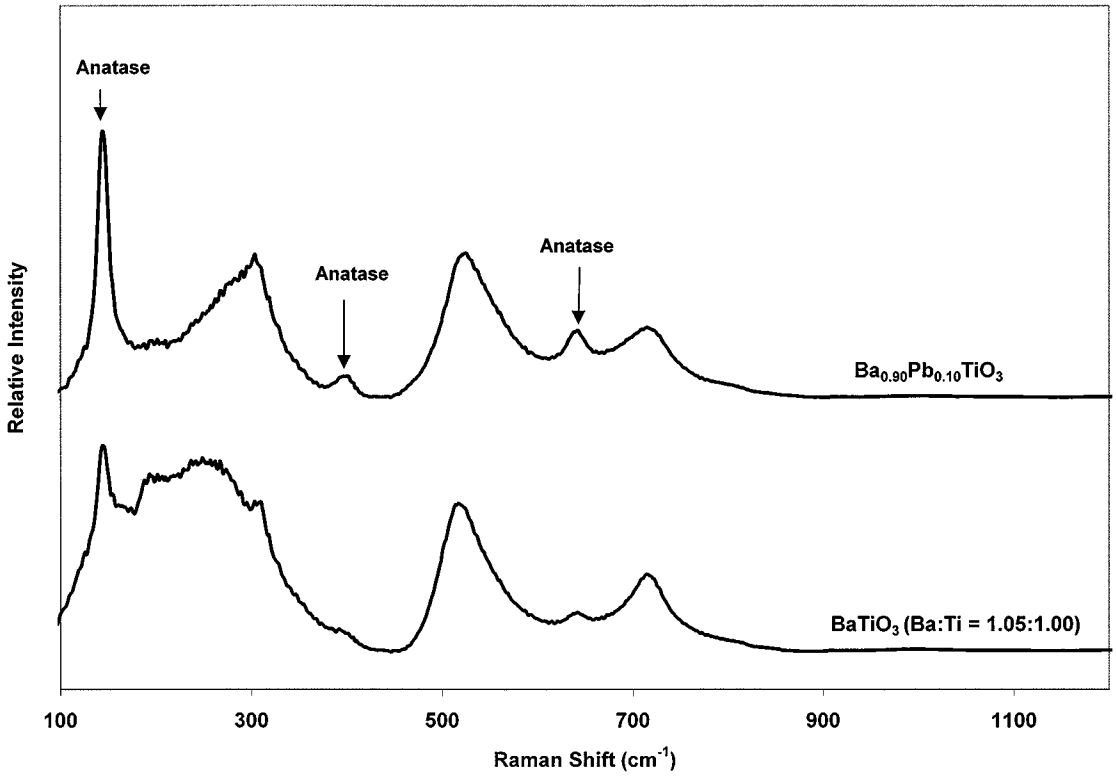

Figure 2 Raman spectrum of hydrothermally synthesized barium titanate and 10% Pb doped barium titanate.

were $a = 4.0004$ Å and $c = 4.0170$ Å. This resulted in a c/a ratio of 1.004, which compared to values in the literature for the particles in the 100–1000 nm size range [12, 13, 24].

Raman data were collected in addition to diffraction data, because Raman spectroscopy can detect lower concentrations of impurity phases and is more sensitive to non-crystalline phases than XRD. In addition, Raman can also distinguish more readily between crystalline phases possessing different symmetries with similar lattice constants, as is the case for $BaTiO_3$ [25]. Fig. 2 shows the Raman data collected, using the Kr+ laser, for the barium titanate sample ($Ba:Ti = 1.05:1.00$) and the sample doped with 10% Pb. Raman peaks at 305 cm^{-1} and 720 cm^{-1} are specific to the tetragonal phase of $BaTiO_3$ [24]. They indicate asymmetry within the TiO_6 octahedra and can be used to distinguish between the cubic and tetragonal symmetry [24]. As can be seen from Fig. 2, the Raman spectrum for the pure $BaTiO_3$ sample, shows peaks at $\sim$305 cm^{-1} and at $\sim$715 cm^{-1}, and confirms that the barium titanate sample has tetragonal symmetry. The Raman data also shows some evidence of anatase. The peaks located at 144 cm^{-1}, 397 cm^{-1} and 638 cm^{-1} are attributed to the starting TiO_2 compound [4]. Comparing the data of Figs 1 and 2 confirms that Raman is more sensitive to the presence of residual anatase than XRD.

Fig. 3 gives the electron microscopy results for the same specimen examined by XRD and Raman scattering. As seen in the figure, it appears that the particles

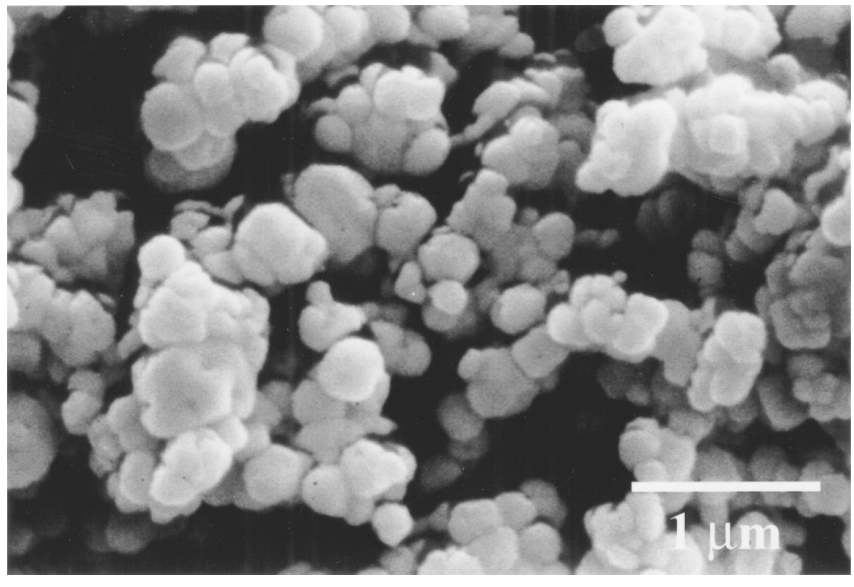

Figure 3 Scanning electron microscopy photomicrograph of pure barium titanate.

are spherical and tend to form agglomerates. Some agglomerates are smaller than others, but overall the individual particles seem to be of similar sizes. The data suggests that the size of individual particles of pure barium titanate is approximately 200 nm. The agglomerate sizes are also consistent with particle size distribution (PSD) measurements, ranging from 100 nm to 1000 nm. The PSD data for the hydrothermally derived barium titanate compared to the commercial $BaTiO_3$ sample. The mean geometric size for the barium titanate sample was ∼400 nm, while that for the commercial sample was ∼450 nm. Because the aerosizer measures the mean geometric diameter of the particles and their agglomerates, the PSD measurements resulted in a mean size that was higher than the individual particle sizes observed by electron microscopy.

Overall, the results showed that excess barium in the starting reaction mixture (Ba : Ti = 1.05 : 1.00) was beneficial in reducing residual anatase and in producing a nearly phase pure tetragonal product. It also compared to commercially available $BaTiO_3$, both in size and phase purity.

As mentioned above, it was hypothesized that the substitution of Pb^{2+} for Ba^{2+} might help stabilize the tetragonal phase. To test this hypothesis, $Ba_{(1-x)}Pb_xTiO_3$ was synthesized at 363 K for 140 h. Under these conditions, it was found that lead incorporated into the structure if the dopant was kept below 20%. This was observed both by XRD and Raman scattering. Fig. 4 shows the XRD patterns for the various lead substituted ($Ba_{(1-x)}Pb_xTiO_3$, $x = 0.05$–0.75) barium titanate powder samples. At higher concentrations of Pb, above 20%, other phases appeared, and at 75% Pb no reaction to the perovskite structure took place. The presence of anatase was also detected at ∼26° 2θ and ∼47° 2θ in each of the samples. Fig. 5 shows the Raman frequency shift of the transverse optic (TO) mode at

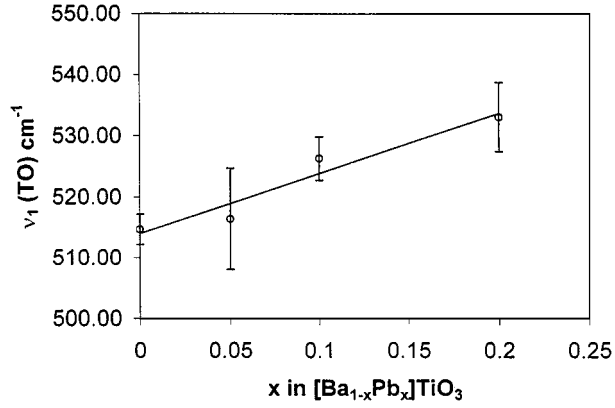

Figure 5 Raman frequency shift for Pb-doped barium titanate.

∼515 cm^{-1}, collected using the Ar-ion laser. The TO mode at ∼515 cm^{-1} shifted to higher frequency as the concentration increased from 0% to 20% Pb. This shift was consistent with Raman data of Burns and Scott [22] for $PbTiO_3 : BaTiO_3$ solid solutions prepared by the conventional high temperature solid state reaction method. The same TO shift was also observed for single crystals, with decreasing temperature on passing through the 4 mm to mm2 transition [23]. The presence of anatase was also detected in the Raman scattering for each of the samples. The anatase concentration increased with increased lead concentration.

Based on the XRD analyses, doping concentrations of 2.5% to 10% Pb seemed to alter the structure of $BaTiO_3$. For the tetragonal symmetry, the 002/200 reflection at ∼45° 2θ will be split with the most intense peak appearing on the *high* angle side of the profile, as seen in Fig. 1 for the calcined commercial sample. However, the reflection at ∼45° 2θ in Fig. 4, has the most intense peak appearing on the *low* angle side for

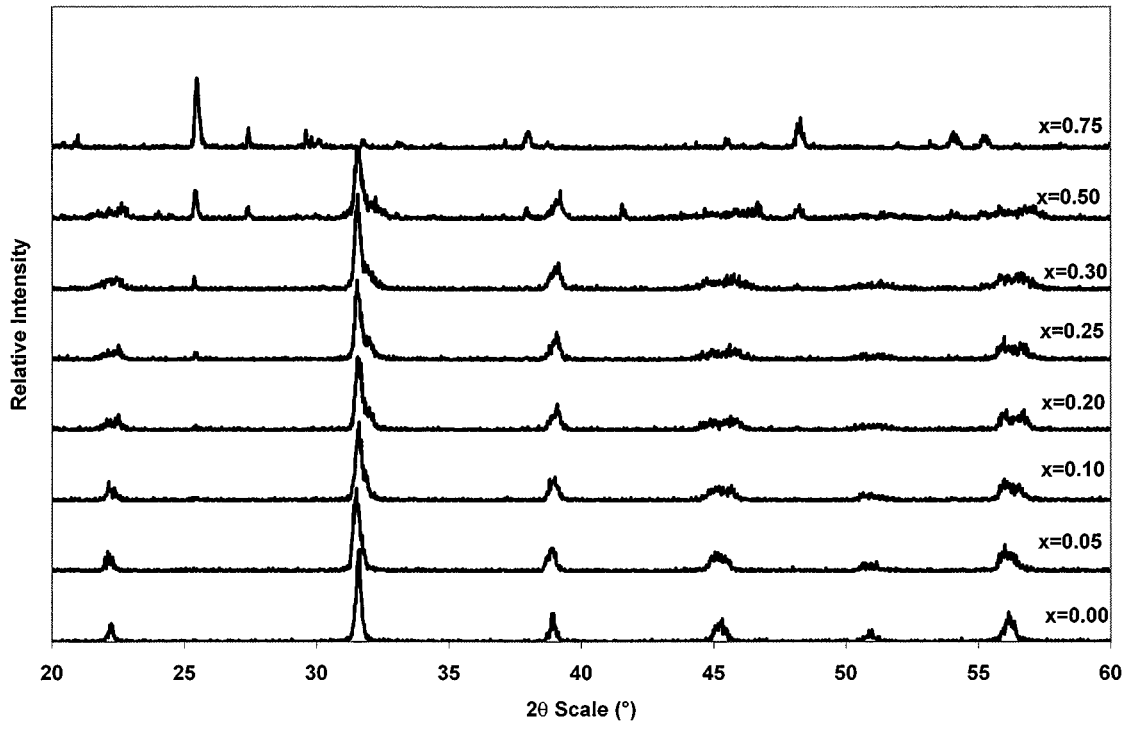

Figure 4 X-ray diffraction patterns for the various Pb-doped barium titanate samples.

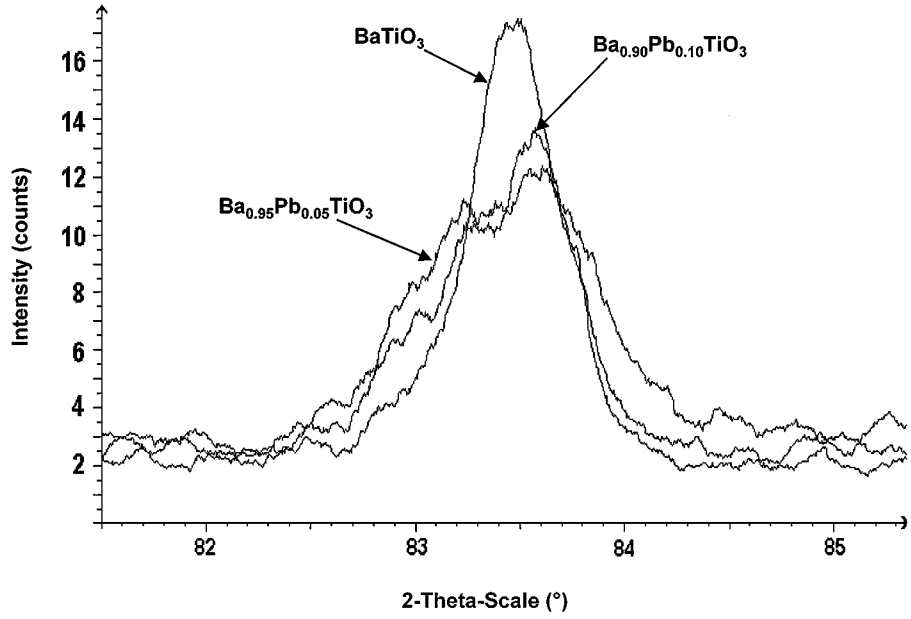

Figure 6 X-ray diffraction patterns of the 222 reflections.

both the 5% and 10% Pb samples. This was not expected for a simple substitutional tetragonal solid solution of the two end member phases. The 222 reflection at $\sim 84^\circ$ 2θ, as seen in Fig. 6, was also asymmetrical and was clearly split for both the 5% and 10% Pb samples. Below 5% dopant the splitting was less obvious but the asymmetry of the peaks were also suggestive of a deviation from tetragonal symmetry. This is evidence of either a mixture of phases, preferred orientation, or of a transition to a phase of different symmetry.

According to the SEM micrographs, the particles were spherical and of similar size. They were agglomerated, but did not show any signs of preferred orientation. Additionally, various XRD samples were prepared using different mounting techniques, and the patterns were identical. It is very unlikely that preferred orientation could be the cause of the apparent deviation in intensity, as expected for the tetragonal phase.

Raman data were also collected for the 10% Pb sample, using the Kr^+ laser, to determine if a lower symmetry phase was obvious. Fig. 2 shows the comparison between the pure barium titanate and the sample doped with 10% Pb. Perry and Hall [24] reported a peak at 196 cm^{-1} for the orthorhombic structure of the pure $BaTiO_3$ system, but from the experimentally obtained Raman data, it was difficult to determine if this peak existed in the doped sample at this wavenumber. Burns and Scott [22] reported Raman data for the $PbTiO_3$-$BaTiO_3$ system, and the experimental pattern for the 10% Pb-doped $BaTiO_3$ was comparable to their results. The spectrum of the 10% Pb sample had a flattened slope starting at ~ 200 cm^{-1} and proceeding to the peak located at ~ 305 cm^{-1}. The pure $BaTiO_3$ sample had a sharper slope and seemed to have additional peaks located in the 200 cm^{-1}–300 cm^{-1} range. There was also a shift to higher frequency of the longitudinal optic (LO) mode at ~ 250 cm^{-1} with increasing lead concentration. According to Perry and Hall [24], this peak at ~ 250 cm^{-1} is sensitive to the crystal structure for the pure $BaTiO_3$ system, so the shift observed in the experimental data might indicate structure differences between the pure barium titanate and the 10% Pb-doped $BaTiO_3$.

From the Raman data it can be concluded that there is a smooth incorporation of Pb as the concentration increases from 0% to 20% Pb; this is based on the TO mode at ~ 515 cm^{-1}. The anatase concentration also increased with increased lead concentration. The presence of anatase was more obvious from the Raman data than XRD. There was a slight indication of a peak at ~ 196 cm^{-1} for the 10% Pb-doped $BaTiO_3$, however, the data did not definitively distinguish between the tetragonal and orthorhombic structure. The peak located at ~ 250 cm^{-1} was shifted to higher frequency as the Pb concentration increased from 0% to 10%. Perry and Hall [24] suggested that this shift was sensitive to the crystal structure, and might therefore indicate structure differences between the pure barium titanate and 10% Pb-doped sample.

In order to better determine if a mixture of phases coexisted, theoretical patterns were generated using Powdercell, a crystal structure visualizer and powder pattern calculation and refinement software package (version 2.1) [26]. The inputs to the program were space group number, lattice parameters and angles, Wyckoff positions of the ions and their respective x-, y- and z-positions. Additionally, it was possible to enter fractional site occupancy and the Debye-Waller temperature factor. The space group number, Wyckoff positions and x-, y- and z-positions were obtained from Wyckoff [27]. The lattice parameters were estimated from Pseudo-Voigt fittings of certain reflections, and data were simulated for mixtures of phases, including two coexisting cubic phases, a mixture of tetragonal and cubic and a mixture of tetragonal and orthorhombic phases. The 002/200 reflections of the experimental patterns were fitted using Topas P (version 1.0) [28], a profile fitting and refinement software package. For the

cubic model determinations, the peaks were fitted using the Pseudo-Voigt function and by constraining the profile fitting shape controlling parameter (η) of the two peaks to be equal. This resulted in d-spacings for each of the peak positions and calculated estimates of the lattice parameters for the two cubic models. The 002/200 and 222 reflections were fitted for the tetragonal structure, and for the 10% Pb sample this resulted in lattice parameters of $a = 3.9771$ Å and $c = 4.0242$ Å. In order to predict the model pattern for the orthorhombic structure, the a, b and c lattice parameters need to be calculated. Since the pattern was assumed to be orthorhombic, the 002/200 reflections in the tetragonal crystal corresponded to the 022/200 reflections in the orthorhombic phase. Likewise, the 222 reflection in the tetragonal phase corresponded to the 240/204 peaks of the orthorhombic symmetry. The lattice parameters obtained for the orthorhombic model were $a = 3.9971$ Å, $b = 5.7177$ Å and $c = 5.6649$ Å. These particular models of the mixed phases, however, did not fit the experimental data for the samples containing Pb additions. It was particularly obvious in the intensity profiles of the {h00} family of reflections of the two coexisting cubic phases. The intensity profiles for the other symmetry mixtures also differed significantly from the experimental data, so it appeared that a mixture of phases did not exist in the low Pb-dopant samples.

Theoretical patterns were also simulated for pure tetragonal and pure orthorhombic phases of Pb-doped barium titanate over the total 2θ range of 20°–150°. Fig. 7a shows a portion of the refinement using the orthorhombic model, and how well it fits the experimental data for barium titanate doped with 10% Pb. Space group Amm2 was used for the orthorhombic model and the atom positions were obtained from Wyckoff [27]. The orthorhombic model appeared to fit the intensity profiles, while the tetragonal model, using space group P4 mm, as shown in Fig. 7b, did not fit as well. This was particularly obvious in the {h00} family of reflections. The tetragonal model had the most intense peak appearing on the *high* angle side, while the orthorhombic model had the most intense peak appearing on the *low* angle side, which was consistent with the experimentally obtained XRD-patterns for low Pb-concentrations. It was therefore believed that the range of 2.5%–10% Pb-doped barium titanate, exhibited orthorhombic character.

A number of studies have shown that the symmetry of $BaTiO_3$ is affected, as the particle size is reduced [7, 12, 13, 16–18]. The present observation of orthorhombic symmetry at room temperature is consistent with previous studies that showed that the orthorhombic-teragonal phase transition shifts up through room temperature with decreasing particle size [18]. Although the precise origin of these effects remains unclear, the

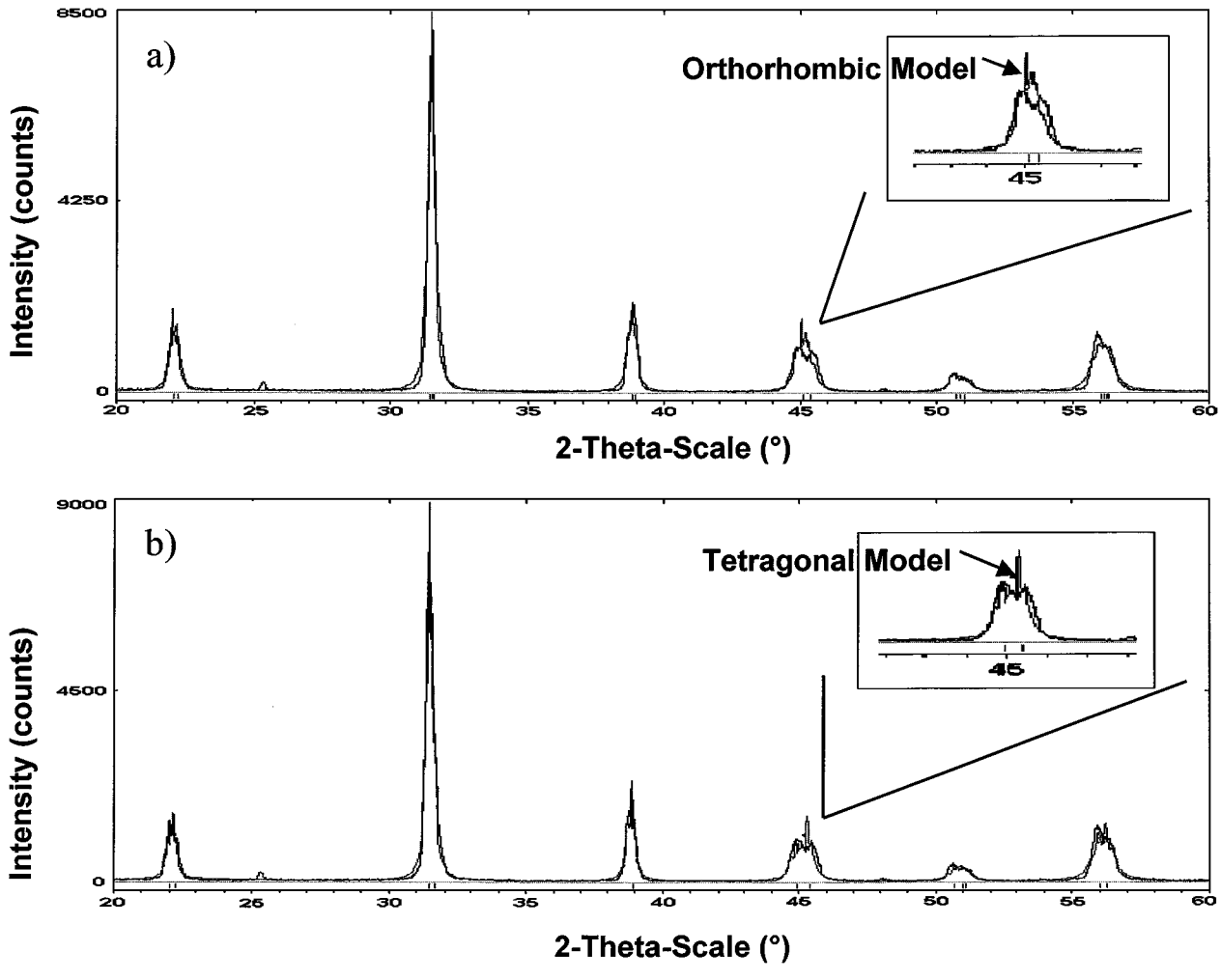

Figure 7 Refinement of x-ray diffraction pattern for the 10% Pb-doped barium titanate (a) Orthorhombic model and (b) Tetragonal model.

symmetry changes may be related in part to a change in the external elastic boundary conditions exerted on the particles [17, 18]. The incorporation of Pb^{2+} induces additional structural distortions that may alter the temperature dependence of the symmetry-particle size relationship. It is possible that the lower symmetry phases shift to higher temperatures due to the combined effects of fine particle size acting together with intrinsic elastic forces generated by the substitution of Pb^{2+}. As noted previously, for large particles under equilibrium conditions at room temperature, one expects a complete substitutional solid solution in the tetragonal phase. Complete tetragonal solid solution has in fact been demonstrated for hydrothermally prepared (Ba, Pb)TiO_3 materials by Riman and co-workers [29]. The degree to which the present observation of orthorhombic symmetry and limited solid solubility can be attributed to the specific hydrothermal reaction conditions and reagents used, requires further investigation.

4. Conclusion

An almost phase pure tetragonal $BaTiO_3$ was synthesized hydrothermally at 363 K by the addition of 5% excess barium to the starting materials. However, both XRD and Raman data showed the presence of some unreacted anatase. Additionally, it was shown that under the hydrothermal reaction conditions used, Pb incorporated into the $BaTiO_3$ structure, only if the Pb concentration was kept below 20%. The presence of anatase increased as the Pb concentration increased. $BaTiO_3$ doped with 75% Pb was mostly anatase, so no reaction to the perovskite structure took place. Doping $BaTiO_3$ with 2.5% to 10% Pb appeared to result in an orthorhombic structure. This was deduced from modeling the x-ray diffraction data, by examining the intensity ratios of the {h00} family of reflections, and by demonstrating splitting of the 222 reflection. It was proposed that the unexpected deviation from 4 mm symmetry resulted from lattice distortions associated with the incorporation of the Pb ions, which altered the temperature dependence of the symmetry-particle size relationship, as previously observed by others for undoped $BaTiO_3$ [17, 18].

Acknowledgements

We would like to thank National Aeronautics and Space Administration (NASA) for the support of this study. In particular we would like to acknowledge the Space Products Division (SPD). T. S. acknowledges the support of Professor P. M. Champion through grants from National Science Foundation (MCB 9904516) and National Institutes of Health (AM 35090).

References

1. Business Communication Co. Inc., Norwalk, CT, American Ceramic Society Bulletin 76 (1997) 38.
2. H. F. KAY and P. VOUSDEN, *Phil. Mag.* **40** (1949) 1019.
3. D. HENNINGS and S. SCHREINEMACHER, *Journal of the European Ceramic Society* **9** (1992) 41.
4. I. CLARK, T. TAKEUCHI, N. OHTORI and D. SINCLAIR, *Journal of Materials Chemistry* **9** (1999) 83.
5. R. VIVEKANANDEN and T. R. N. KUTTY, *Powder Technology* **57** (1989) 181.
6. P. K. DUTTA and J. R. GREGG, *Chemistry of Materials* **4** (1992) 843.
7. E. SHI, C. XIA, W. ZHONG, B. WANG and C. FENG, *J. Amer. Ceram. Soc.* **80** (1997) 1567.
8. R. VIVEKANANDEN, S. PHILIP and T. R. N. KUTTY *Materials Research Bulletin* **22** (1986) 99.
9. D. HENNINGS, G. ROSENSTEIN and H. SCHREINEMACHER, *Journal of the European Ceramic Society* **8** (1991) 107.
10. S. WADA, T. SUZUKI and T. NOMA, *Journal of the Ceramic Society of Japan*, International Edition **103** (1995) 1207.
11. *Idem., ibid.* International Edition **104** (1996) 364.
12. K. UCHINO, E. SADANAGA and T. HIROSE, *Communications of the American Ceramic Society* **72** (1989) 1555.
13. X. LI and W. SHIH, *J. Amer. Ceram. Soc.* **80** (1997) 2844.
14. J. O. ECKERT, C. C. HUNG-HOUSTON, B. L. GERTSEN, M. M. LENCKA and R. E. RIMAN, *ibid.* **79** (1996) 2929.
15. A. NØRLUND CHRISTENSEN and S. E. RASMUSSEN, *Acta Chemica Scandinavica* **17** (1963) 845.
16. B. BEGG, K. FINNIE and E. VANCE, *J. Amer. Ceram. Soc.* **79** (1996) 2666.
17. G. ARLT, D. HENNINGS and G. DEWITH, *J. Appl. Phys.* **58** (1985) 1619.
18. M. H. FREY and D. A. PAYNE, *Physical Review B* **54** (1996) 3158.
19. G. SHIRANE, R. PEPINSKY and B. C. FRAZER, *Acta Crystallographica* **9** (1956) 131.
20. G. SHIRANE and A. TAKEDA, *Journal of the Physical Society of Japan* **6** (1951) 329.
21. Aerosizer User manual, Amherst Process Instruments Inc., Hadley, MA (1995).
22. G. BURNS and B. A. SCOTT, *Solid State Communications* **9** (1971) 813.
23. *Idem., Physical Review B* **7** (1973) 3088.
24. C. H. PERRY and D. B. HALL, *Physical Review Letters* **15** (1965) 700.
25. L. H. ROBINS, D. L. KAISER, L. D. ROTTER, P. K. SCHENCK, G. T. STAUF and D. RYTZ, *J. Appl. Phys.* **76** (1994) 7487.
26. Powdercell software version 2.1, Created by Werner Kraus and Gert Nolze at the Federal Institute for Material Research and Testing (BAM), Unter den Eichen 87, D-12205 Berlin, Germany (1999).
27. R. W. G. WYKOFF, "Crystal Structures" (Interscience Publishers, New York, 1967) p. 405.
28. Topas P software version 1.0, DIFFRAC plus package, Bruker AXS GmbH, Written by Alan A. Coelho, Michael Jacob and Thomas Taut (1998).
29. R. E. RIMAN, private communications.

Received 21 December 1999
and accepted 31 July 2000